Coulomb Energy Shifts in the $A = 18$ Nuclei*

S. Kahana

Brookhaven National Laboratory, Upton, New York 11973

(Received 17 June 1971)

The energies of the lowest five $T = 1$ states in F^{18} and Ne^{18} are predicted on the basis of a calculation (a) using a realistic force tuned to fit the O^{18} members of the same multiplets and (b) including the known Coulomb interactions between protons. The nucleons are permitted to be in the $1d_{5/2}$ and $2s_{1/2}$ levels, the latter being described by Woods-Saxon wave functions. Particle-particle, hole-particle, and hole-hole corrections are included. Reasonable agreement with experiment is obtained for all but the excited 0^+ multiplet. It is necessary to introduce a small (short ranges and attractive) charge-dependent force to explain the F^{18} data.

I. INTRODUCTION

In an earlier paper[1] the interplay between Coulomb forces and nuclear residual interactions was considered in relation to the ground-state energy differences between the calcium and scandium isotopes. These analog displacement energies were obtained in a perturbative fashion including a term which was first-order in both the nuclear residual interactions and the Coulomb interaction. The detailed calculations relied strongly on a $(f_{7/2})^n$ model and hence were not greatly sensitive to the nature of the single-particle orbitals used. The deeply bound $f_{7/2}$ neutron is only weakly perturbed by the introduction of the Coulomb potential. The present work extends this earlier treatment in several directions. First, the nuclei considered in most detail involve a pair of nucleons outside an O^{16} rather than a Ca^{40} core, and the shell-model space is broadened to include two single-particle levels. The $2s_{1/2}$ level, which plays an important role in the low-lying states of the mass-18 nuclei, is highly volatile with respect to the change of a neutron into a proton. The mean square radius for a nucleon in such a level increases from 17 fm^2 for a neutron to about 25 fm^2 for a proton. Hopefully this volatility can be exploited to magnify the mixed nuclear-Coulomb effects concentrated on here. Secondly, the present calculations have been enlarged to encompass all three members of a given isotopic spin ($T = 1$) multiplet; and because of the broadened model space, analog-state displacement energies may be considered for more than just the ground states. Thus the Coulomb-energy displacements of the lowest five $T = 1$ states in both F^{18} and Ne^{18} are considered, and a large increase is made in the experimental data brought under scrutiny. Finally, an estimate is made in these finite nuclei of the effect of a charge-dependent nuclear force other than that due to the Coulomb interactions. There is, of course, evidence

for such a force in the free two-nucleon system, but from this work there is apparently also some systematic evidence in the $A = 18$ and 42 $T = 1$ multiplets.

The over-all philosophy adhered to has not changed from that expressed earlier.[1] It is expected that energies which derive from a combination of Coulomb and nuclear interactions are more sensitive to the specific spatial structure of the residual nuclear force than are the purely nuclear energies. Matrix elements of the nuclear force from the model space to much more highly excited states play an important role, perhaps allowing one to detect the presence of a repulsive core. To perform the calculations of the following sections of this paper the usual picture of the shell model must be altered somewhat. Neutrons and protons cannot be described by the same wave functions, e.g., oscillators. It is just from such differences that our effects arise, and consequently more realistic wave functions are used.[2]

II. SINGLE-PARTICLE ENERGIES AND WAVE FUNCTIONS

The choice of single-particle wave functions to be used in Coulomb-energy calculations is, in principle, straightforward. To treat two valence particles outside closed shells a realistic well may be fitted to the known proton and neutron single-particle energies. (Few hole nuclei may be treated in a parallel fashion.) In considering the proton and neutron energies simultaneously, one is, of course, determining a Coulomb energy between particle and core and, hence, inferring a radius for the orbit of this particle. Unfortunately, in practice, these radii turn out to be rather small,[3] and although a tentative solution to this problem has been suggested,[4] the situation is at present unclear.[5] Nevertheless, by constructing the particle wells with empirical single-particle energies and under the constraint of reasonable

geometry, one can bypass the difficulties encoun-
tered for a single valence nucleon. The sensi-
tivity of the two-particle results to the choice of
single-particle wave functions is then easy to ex-
plore, and is found to be rather weak. In partic-
ular, only the choice of well for the $2s_{1/2}$ level in
the $A=18$ nuclei is under question, the $d_{5/2}$ level
being in the present context quite deeply bound.

In Fig. 1 are shown the experimental energies
of the single-particle levels to be used in the pres-
ent calculation. The change in the $1d_{5/2}$-$2s_{1/2}$
splitting between O^{17} and F^{17}, referred to as a
Thomas-Ehrman shift,[6] is presumably a conse-
quence of the lower Coulomb energy between pro-
ton and core for the more extended $2s_{1/2}$ state.
The rather large shift, ~370 keV, should be re-
flected in differences between the spectra of Ne^{18},
F^{18} on the one hand and the spectrum of O^{18} on the
other. One might ask whether the extra binding
due to residual interactions between the two va-
lence nucleons in mass-18 nuclei demands the use
of more deeply bound single-particle levels and
hence use of a reduced Thomas-Ehrman shift.
This raises the issue of the asymptotic form of
the two-valence-nucleon wave function, which
will be dealt with more completely in the next
section. However, at this stage it is easy enough
to examine the relation between binding energy
and Coulomb energy for the valence nucleons.
Briefly, for a reasonable choice of binding ener-
gies for the $1d_{5/2}$ and $2s_{1/2}$ levels the shift remains
appreciable. The low-angular-momentum noded
character of the $2s_{1/2}$ wave function is decisive,
causing the wave function to extend outwards
radially.

A Woods-Saxon central well and a conventional
Thomas spin-orbit potential are used for the
charge-independent part of the single-particle
potential. The Coulomb interaction between a
valence proton and the closed core is approxi-
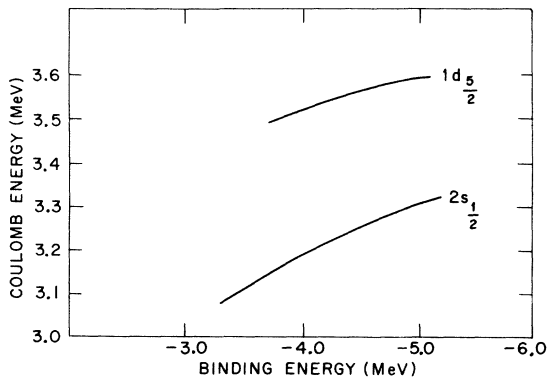mated by that due to a uniform distribution of

charge, with the radius being obtained from elec-
tron scattering analysis. In the mass-17 nuclei
the simplest way to circumvent the difficulty pre-
viously referred to is to ignore the exchange Cou-
lomb energy between valence and core protons.
This leads to reasonable radii for both the $1d_{5/2}$
and $2s_{1/2}$ valence orbits, radii well outside the
inner core. Well parameters are given in Table
I which directly predict the experimental proton
and neutron binding energies for the $2s_{1/2}$ and
$1d_{5/2}$ states in O^{17} and F^{17}. Thus in principle, all
single-particle effects such as the exchange en-
ergies, n-p mass difference, etc., are included.
The predicted energies as well as the implied
Coulomb energies are also listed in this table.
The diffusivity and spin-orbit strength were fixed
at $a=0.63$ fm and $V_{so} = 5.7$ MeV for these and all
future wells used in this work. Despite the rath-
er small radius parameter $r_0 = 0.975$ fm used for
the $2s_{1/2}$ nucleon in the above wells, the resulting
neutron and proton $2s_{1/2}$ orbits have rms radii of
~4.0 and 5.0 fm, respectively.

The two-particle calculations carried out in the
remainder of this work relied basically on the
wells in Table I. However, other single-particle
potentials, listed in Table II, were constructed
to check the sensitivity of the two-particle ener-
gies to an increase in the single-particle binding
energies. The wells in Table I which led to the
"correct" direct Coulomb energies had different
radii and depths for the s and d levels. Relaxing
the constraint on the Coulomb energy permits one
to place the two levels in similar wells (Table II).
In Fig. 2 is shown the variation of the d and s

TABLE I. Parameters for the nuclear single-particle
well

$$U = -V_0 f(r) + \left(\frac{\hbar}{m_\pi c}\right)^2 \vec{1} \cdot \vec{\sigma} \left|\frac{d}{dr} f(r)\right|,$$

with $f(r) = -V_0[1+e^{(r-r_0 A^{1/3})/a}]^{-1}$. This charge-indepen-
dent part of the well is selected to give the correct neu-
tron binding energies for the $1d_{5/2}$ and $2s_{1/2}$ levels, and
also give the correct proton energies when the potential
of a uniform charge distribution, radius 3.497 fm, is
added. Also given are the calculated proton and neutron
binding energies, E_p, E_n, and the Coulomb energies, E_C.
The calculated difference in Coulomb energies, 0.367
MeV, agrees well with the experimental difference of
0.370 MeV.

	$2s_{1/2}$	Expt.	$d_{5/2}$	Expt.
V_0 (MeV)	74.5030		57.0744	
r_0 (fm)	0.975		1.17	
E_p (MeV)	−0.0970		−0.600	
E_n (MeV)	−3.270		−4.140	
E_C (MeV)	+3.173	3.172	3.539	3.542
$E_C(d) - E_0(s)$ (MeV)	0.367	0.370		

FIG. 1. Single-particle splittings in O^{17} and F^{17}.

Coulomb energies with neutron binding energy for a fixed well size parameter $r_0 = 1.17$ fm. From this figure it is easily seen that the Thomas-Ehrman shift is appreciable for any reasonable choice of binding energy.

As a footnote to this section one might note that a perturbative calculation of the proton Coulomb energies is excellent for the d level and reasonable for the s level. Table III compares the direct Coulomb energies obtained for the s and d levels calculated exactly and in first-order perturbation theory. A consistent calculation of the two-particle energies can be made if the Coulomb and nuclear residual interactions are treated perturbatively. For example, one should not carry the iteration of the Coulomb potential past first order in the calculation of the single-particle wave functions. Table III suggests that this limitation would not lead to serious error. In the later calculations of two-particle interactions we will, in general, rely on perturbation theory, estimating the size of all terms up to a given order and occasionally including some higher-order terms.

III. TWO-VALENCE NUCLEONS

A. Formal Theory

If the valence-nucleon interaction is derived from the usual reaction-matrix theory,[7] an effective two-particle wave function may be defined by

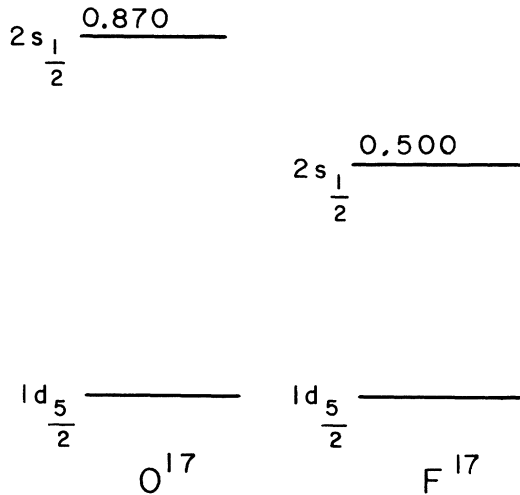$$\Psi = \Phi + \frac{Q}{E_0 - H_0} K(E)\Phi \cdots , \tag{1}$$

FIG. 2. Variation of the Coulomb energy of the $2s_{1/2}$ and $1d_{5/2}$ levels with the neutron binding energies of these states. An appreciable difference between the s and d Coulomb energies obtains for the range of binding energies shown.

TABLE II. Identical to Table I with changes made so as to: (a) use the same geometry for the s and d levels, and (b) deepen the neutron binding energies.

	$2s_{1/2}$	$1d_{5/2}$
V_0 (MeV)	59.3988	59.1829
r_0 (fm)	1.17	1.17
R_C	3.497	3.497
E_n	−4.14	−5.14
E_p	−0.92975	−1.54668
$E_p(s) - E_p(d)$ (MeV)	0.617	

where Φ is the unperturbed wave function in a model valence space, $K(E)$ is the Brueckner reaction matrix, Q a projection operator out of states occupied in the closed core or in the model valence space. Also $H_0 = H_0(1) + H_0(2)$ is the shell-model Hamiltonian obtained, presumably, in a self-consistent fashion. For a pair of nucleons outside of an isospin-zero $(T = 0)$ core, the wave function may be written $\Psi(T, T_z)$ with $T = 1$ and $T_z = 1, 0, -1$ for the two-neutron (nn), neutron-proton (np), and two-proton (pp) nuclei, respectively. If both $K(E)$ and H_0 are derived from charge-independent forces then the energies E derived from Eq. (1) are, of course, independent of T_z. The Coulomb interaction may be introduced at this stage and evaluated perturbatively. An approximate separation of the Coulomb interaction into a one-body and a two-body part is possible:

$$V_C = V_C(1) + V_C(2) + v_C(1, 2)$$

$$= V_C(\vec{r}_1)\frac{1 - \tau_z(1)}{2} + V_C(\vec{r}_2)\frac{1 - \tau_z(2)}{2}$$

$$+ \frac{e^2}{|\vec{r}_1 - \vec{r}_2|}\frac{[1 - \tau_z(1)][1 - \tau_z(2)]}{4} . \tag{2}$$

Here $V_C(\vec{r})$ is the single-particle potential arising from the known distribution of charge in the unperturbed core. The aim of this paper is to

TABLE III. Coulomb energies calculated "exactly" from Tables I and II, and in perturbation theory.

	d	s
(a) $E_n(s) = -3.27$, $E_n(d) = -4.14$		
E_C (exact)	3.539	3.173
E_C (perturbation)	3.549	3.273
(b) $E_n(s) = -4.14$, $E_n(d) = -5.14$		
E_C (exact)	3.593	3.210
E_C (perturbation)	3.595	3.274

calculate the energy

$$\Delta E(T_z) = \langle \Psi(T, T_z) | V_C | \Psi(T, T_z) \rangle$$

$$= \langle \Phi | V_C(1) + V_C(2) | \Phi \rangle + \langle \Phi | v_C(1, 2) | \Phi \rangle + \langle \Phi | K(E) \frac{Q}{E - H_0} [V_C(1) + V_C(2)] | \Phi \rangle$$

$$+ \langle \Phi | [V_C(1) + V_C(2)] \frac{Q}{E - H_0} K(E) | \Phi \rangle + \langle \Phi | K(E) \frac{Q}{E - H_0} [V_C(1) + V_C(2)] \frac{Q}{E - H_0} K(E) | \Psi \rangle$$

$$+ \langle \Phi | K(E) \frac{Q}{E - H_0} v_C(1, 2) | \Phi \rangle + \langle \Phi | v_C(1, 2) \frac{Q}{E - H_0} K(E) | \Phi \rangle$$

$$+ \langle \Phi | K(E) \frac{Q}{E - H_0} v_C(1, 2) \frac{Q}{E - H_0} K(E) | \Phi \rangle . \tag{3}$$

The wave function Φ which is constructed from wave functions of the charge-independent Hamiltonian H_0 may be regarded as the model function for the two-neutron member of the $T = 1$ multiplet. Thus the first two terms on the right side of Eq. (3) are immediately identifiable as the lowest-order model-space contribution to the Coulomb energy and may be evaluated using neutron radial wave functions. The third and fourth terms are mixed-perturbative in both the nuclear residual and Coulomb interactions. Since these latter terms involve only the single-particle part of the Coulomb force, they may be viewed as charge-
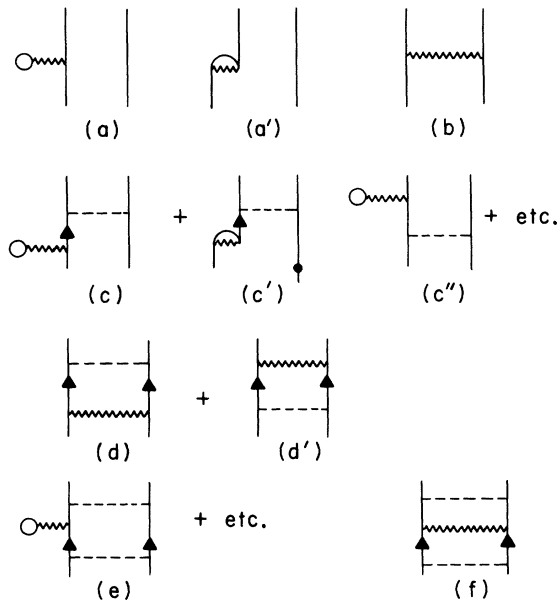

FIG. 3. (a)–(f) Diagrammatic representation of energies in Eq. (3). A wavy line stands for a Coulomb interaction, a dashed line a nuclear residual interaction. A closed loop corresponds to an interaction with the nucleons in the closed core. If antisymmetry is preserved, exchange energies like those in (a′) and (c′) are in principle included.

dependent corrections to the nuclear residual interaction due to changing neutron radial wave functions into proton functions.[1] The remaining terms in Eq. (3) are regarded in this work as essentially small, but will be discussed in detail.

To clarify the interpretation of the various terms in Eq. (3) we present diagrammatic representations in Fig. 3. The complete set of terms occurs only for the pp nucleus; in the np case one of the single-particle potentials, $V_C(i)$, and the two-particle Coulomb potential, $v_C(1, 2)$, are inoperative Figures 3(a) and 3(b) correspond to the first two terms in Eq. (3), while Figs. 3(c), 3(c″), etc., are the mixed nuclear-Coulomb terms discussed in Ref. 1 and concentrated on here. It is easy to complete the correspondence of terms in Eq. (3) and diagrams in Fig. 3.

The Bethe-Goldstone Eq. (2)[7] does not, however, represent the entire perturbation series for the two-valence-nucleon energy. In Fig. 4 are exhibited a series of terms not described by this equation but which are proper contributions to the energy. Together Figs. 3 and 4 contain all contributions of first order in the Coulomb interaction and of first order in the nuclear residual interaction. Some terms of second order in $K(E)$ which are considered important are also included. The projection operator Q in Eq. (2) implies that the intermediate states in Fig. 3(c) are "particle" states, i.e., unoccupied in the mass-18 nuclei. Terms like those shown in Fig. 4(a), with intermediate "hole" states, must also be included to complete the conversion of the neutron into proton radial functions. The exchange terms shown in Fig. 3(c′) and Fig. 4(a′) are expected to be small but must be included to the order considered. As indicated earlier leaving out the contribution of Fig. 3(a′), the lowest-order Coulomb exchange energy, is an effective way of guaranteeing reasonably sized single-particle orbitals. Many other exchange corrections are included, however, by the use of antisymmetrized nuclear and Coulomb interactions.

The diagrams of Fig. 3(d) and Fig. 4(b) which results from two-particle and four-particle–two-hole intermediate states may be considered as modifications to the direct Coulomb energy between the pair of valence protons in Ne^{18}. Since the residual interaction $K(E)$ is on the whole attractive, these latter terms are likely to result in an increase in the Coulomb energy. The terms shown in Figs. 3(e) and 4(c) are quadratic in the nuclear residual interaction but should not be ignored, since they contain Coulomb interactions diagonal in the intermediate states, unlike the similar term Fig. 3(f) which is very small. Finally, the particle-hole contributions of Fig. 4(e) are naturally included in our calculations because of the manner in which $K(E)$ is later defined, while Fig. 4(d) is calculated explicitly.

In a strict perturbative treatment the energy E in the denominators of Eqs. (2) and (3) should be the unperturbed energy $E = E_0(1) + E_0(2)$ arising from H_0. The extra binding energy due to the interaction of the valence particles alters the asymptotic behavior of the wave function Ψ. As demonstrated in Ref. 1, use of the unperturbed energy E_0 in evaluating the contributions of Figs. 3(c), 3(c'), 4(a), 4(a'), etc., accounts for this modified behavior to first order in $E - E_0$. It is difficult to correct for the asymptotic behavior of Ψ consistently to higher order, but redoing the basic calculations with deeper single-particle levels mocks up this behavior to some extent.

A comprehensive calculation of all corrections, relying on harmonic-oscillator wave functions, is presented later. First, we give the results of a Woods-Saxon calculation for what are expected to be the major contributions to the analog displacement energies, i.e., Figs. 3(a), 3(b), 3(c), 3(c''), etc., and Figs. 4(a), 4(a').
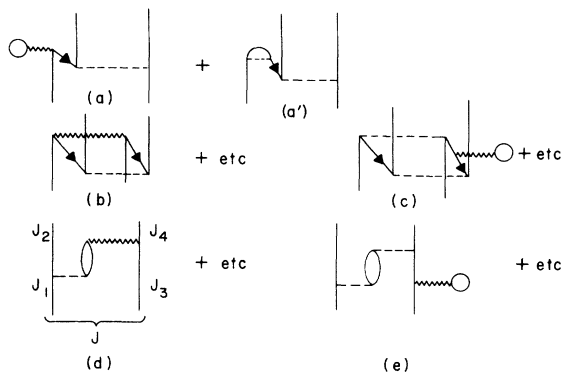

FIG. 4. (a)–(e) Additional contributions to the Coulomb energy shifts in the $T_z = 0, -1$ nuclei. The diagrams in Fig. 4 involve hole contributions (backward-going arrows) in intermediate states, i.e., breaking up the doubly magic core.

B. Explicit Calculations

The general calculation outlined in the next few paragraphs is, in principle, quite simple. Rather than evaluating the perturbative contributions of Figs. 3(c) and 4(a), the neutron wave functions are converted into their proton counterparts by adding the valence-core Coulomb potential $V(\vec{r}_i)$ to the charge-independent shell-model potential $U(\vec{r}_i)$. The residual interaction $K(E)$ is then diagonalized in the nn, np, pp model spaces, respectively. This slight straying from first-order perturbation theory in the Coulomb interaction is extended to the calculation of the direct Coulomb energy between the pair of valence protons in Ne^{18} [Fig. 3(b)]. The results of a purely perturbative calculation are also given, however.

In practice no model for the nuclear residual interaction has yielded a prediction of the energies of the low-lying states of O^{18} sufficiently accurate for our present purposes. For simplicity we have then adopted a relative s-wave representation of $K(E)$ which has as its main component a "realistic" force derived by Kahana and Tomusiak (KT)[8]:

$$K(E) = -24.00 \left[e^{-0.085(r_{12}/\bar{\lambda}_p)} - 8\pi \left(\frac{\bar{\lambda}_p}{0.085} \right)^3 \right.$$
$$\left. \times 0.015\,29\delta(\vec{r}_{12}) \right] \text{ MeV}, \qquad (4)$$

where $\bar{\lambda}_p = 0.21$ fm is the "barred" proton Compton wavelength. The relevant features of $K(E)$ are that as a free ^1S reaction matrix it fits the proton-proton s-wave scattering data up to 300 MeV, and the short-range repulsive component plays an important role in this fitting. This force does not by itself give the accurate description of O^{18} required. However, the omission of a core-polarization contribution to $K(E)$ in the KT work and of the $d_{3/2}$ single-particle wave function in the present work can be compensated for by a renormalization of the nuclear residual interaction. Since only a prediction of the charge-dependent shifts in energies of two-neutron states are desired, there is no harm in tuning $K(E)$ so as to correctly position the low-lying levels of O^{18}. The core polarization is probably best treated by adding to Eq. (4) a state-dependent long-range interaction. On the other hand, the effect of the neglected $d_{3/2}$ level probably yields a simple multiplicative renormalization. For simplicity the latter approach is followed, although results obtained by additive corrections of $K(E)$ are quite similar.

The final nn matrix elements are displayed in Table IV, along with the factor required to place the lowest-lying 0^+, 2^+, 4^+ states at their proper energies. The 0^+, 2^+ matrix elements have been

increased by similar factors, but the 4^+ element must be reduced in size.[9] The energies of the second 0^+, 2^+ states are then predictions of the renormalized force, and are reasonably well placed. Table IV includes the calculated and experimental binding energies for the five lowest states of O^{18}.

The nn matrix elements have, of course, been calculated using the Woods-Saxon neutron wave functions obtained from the potentials of Table I. The matrix elements employed in a comparable diagonalization of Ne^{18} are obtained by replacing the neutron functions by their proton counterparts and are shown in Table V. To deduce the np matrix elements for F^{18} one can average the nn and pp elements. If first-order perturbation theory in the Coulomb field is good, the np matrix elements may also be obtained from proton-like wave functions calculated in a half-strength Coulomb field.[1] The F^{18} matrix elements obtained from both these procedures are listed in Table V. It is evident that perturbation theory in the Coulomb potential works

reasonably well for the single-particle wave functions. The last ingredient in the np and pp diagonalizations are the appropriate single-particle energies and the direct Coulomb energy in the pp system. These are presented in Table VI with the Coulomb interaction of Fig. 3(b) being given both in strict perturbation theory (nn wave functions) and exactly (pp wave functions). Finally, the results of this straightforward calculation for F^{18} and Ne^{18} are presented in Table VII, first as equivalent two-particle binding energies $B(J_\alpha)$ for a given level J_α and then as what may be considered shifts $\Delta E(J_\alpha)$ from the O^{18} standard energies. For example, the equivalent binding energy of a given F^{18} state is defined so as to remove the binding of a $d_{5/2}$ neutron and a $d_{5/2}$ proton,

$$B(J_\alpha, F^{18}) = E(J_\alpha, F^{18}) - E(G.S., O^{16})$$

$$- [E(G.S., F^{17}) - E(G.S., O^{16})]$$

$$- [E(G.S., O^{17}) - E(G.S., O^{16})]. \qquad (5)$$

TABLE IV. The neutron-neutron matrix elements of the renormalized nuclear force. J-dependent renormalizations of $K(E)$ used to obtain the above matrix elements are also listed as are the calculated and experimental energy levels. The energies are given relative to zero energy for an unperturbed $(d_{5/2})^2$ pair, and the single-particle separations used are listed.

State label	Matrix element (MeV)	Renormalization factor	Single-particle energy
	$J = 0^+$		
$(d^2)^2$	−3.1744	1.600	0.00
d^2s^2	−1.4448	1.600	
$(s^2)^2$	−2.7760	1.600	1.74
	$J = 2^+$		
$(d^2)^2$	−0.8843	1.500	0.00
$d^2(ds)$	−1.0016	1.500	
(ds)	−1.8228	1.500	0.87
	$J = 4^+$		
$(d^2)^2$	−0.3500	0.6971	0.00

State	Calculated energies	Experimental energies
	$J = 0^+$	
0_2^+	−0.308	−0.268
0_1^+	−3.903	−3.902
	$J = 2^+$	
2_2^+	0.084	0.014
2_1^+	−1.921	−1.922
	$J = 4^+$	
4^+	−0.350	−0.350

TABLE V. Two-proton (Ne^{18}) and neutron-proton (F^{18}) matrix elements obtained by replacing the appropriate neutron wave functions by proton counterparts. The F^{18} matrix elements are calculated by (a) averaging the nn and pp elements, and (b) by reducing the core charge from 8 to 4 in the Coulomb part of the proton potential.

Angular momentum J	State	$Ne^{18}(pp)$	Matrix elements F^{18} (averaged nn and pp)	F^{18} $(V_C \sim \frac{1}{2}Z)$
0^+	$(d)^2$	-3.1139	-3.1441	-3.1528
0^+	$d^2 s^2$	-1.3104	-1.3776	-1.4016
0^+	$(s^2)^2$	-2.4618	-2.6189	-2.6792
2^+	$(d^2)^2$	-0.8616	-0.8729	-0.8754
2^+	$d^2(ds)$	-0.9381	-0.9699	-0.9800
2^+	$(ds)^2$	-1.6475	-1.7352	-1.7616
4^+	$(d^2)^2$	-0.3377	-0.3439	-0.3448

The quantities $E(J_\alpha, F^{18})$ are total binding energies adjusted for np mass differences, and G.S. stands for ground state. Similarly quantities $B(J_\alpha)$ can be defined for Ne^{18}, and of course O^{18}, with neutrons and protons being interchanged suitably. As defined, $B(J_\alpha, F^{18})$ will generally differ only slightly from the corresponding quantities $B(J_\alpha, O^{18})$, while $B(J_\alpha, Ne^{18})$ will contain an extra effective two-particle Coulomb energy. The energy shifts defined by

$$\Delta E(J_\alpha, F^{18}) = B(J_\alpha, F^{18}) - B(J_\alpha, O^{18}) \tag{6}$$

then are small, perhaps $\lesssim 100$ keV, while

$$\Delta E(J_\alpha, N^{18}) = B(J_\alpha, N^{18}) - B(J_\alpha, O^{18}) \tag{7}$$

are expected to be of the order of 400 keV. The calculated binding energies $B(2_2^+)$ and $B(0_2^+)$ for Ne^{18} and F^{18} will reflect residual inaccuracies in the predictions for these "second" excited states in O^{18}, but the energy shifts $\Delta E(J_\alpha)$ will have these inaccuracies removed.

Also contained in Table VII are the experimental values of $\Delta E(J_\alpha)$, $B(J_\alpha)$.[10, 11] The predictions are good, with the uniform exception of the excited 0_2^+ state. It is easy to trace the unwanted downward displacements of the 0_2^+ state by about 200 keV in F^{18} and 500 keV in Ne^{18}. This state, which is $\sim 75\%$ $(2s_{1/2})^2$, has been depressed by the large (370-keV) Thomas-Ehrman shift between the s and d levels in F^{17}. To some extent the same illness afflicts the 2^+ states in Ne^{18}, which in our calcu-

lations are more than 50% (ds). The spectacular failure of these simple calculations for the excited 0^+ states indicates one of two things: either this state is not well described by the $(2s_{1/2}, 1d_{5/2})$ model space, or our treatment of the single-particle energies is inadequate. The answer is probably found in a combination of these two features. This rather interesting and disturbing point will be discussed later.

For all but the maverick 0^+ state, the shifts $\Delta E(J_\alpha)$ are within 100 keV or so of their experimental values. Since there is a series of corrections yet to be included, we do not wish here to dwell on the accuracy of the predictions.

TABLE VI. The single-particle energies used in diagonalizing F^{18} and Ne^{18} energy matrices. Also shown are the direct Coulomb energy [Fig. 3(b)] calculated in Ne^{18} using two-proton wave functions ("exact") or two-neutron wave functions (perturbative).

J	State	Single-particle energies (MeV)	Coulomb matrix elements (pp)	(nn)
		F^{18}		
0^+	d^2	0.000		
	s^2	1.370		
2^+	d^2	0.000		
	ds	0.685		
4^+	d^2	0.00		
		Ne^{18}		
0^+	$(d^2)^2$	0.000	0.4547	0.4748
	$d^2 s^2$		0.0438	0.0494
	$(s^2)^2$	1.000	0.3082	0.3643
2^+	$(d^2)^2$	0.000	0.3880	0.4043
	$d^2(ds)$		0.0286	0.0313
	$(ds)^2$	0.500	0.3425	0.3744
4^+	d^4	0.000	0.3625	0.3773

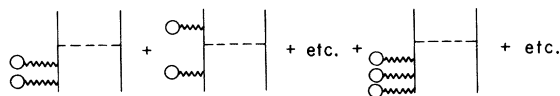
FIG. 5. Some contributions to Coulomb energy shifts arising from iterating the Coulomb potential past first order in the nuclear wave functions.

C. Corrections

This is an appropriate point at which to calculate the contributions from the remaining diagrams of Figs. 3 and 4. The energies from Fig. 3(a), 3(b), 3(c) have, of course, been included, but not in a perturbative fashion. As demonstrated in columns 4 and 5 of Table V, the inclusion with Fig. 3(c) of terms such as those shown in Fig. 5 is probably unimportant. However, if Fig. 3(b) were taken literally, the proton-proton Coulomb energies in column 4, Table VI would be replaced by those in column 5 of the same table. The effect of such a change is shown in column 5 of Table VII. Of course, the results of F^{18} are unchanged by this latter consideration.

Of all the terms shown in Figs. 3 and 4, the most tedious to calculate are the particle-hole

corrections in Fig. 4(d). The particle-particle and hole-hole corrections [Figs. 3(d), 3(e), 4(b), 4(c)] require no angular momentum recoupling and are relatively easy to obtain. In all calculations of corrections, harmonic-oscillator wave functions were employed appropriate to an oscillator constant $\hbar\omega = 13.4$ MeV. The force used differed from Eq. (4) slightly in the nature of its repulsive term. The strength of this force was readjusted to give oscillator-Woods-Saxon equality within the model space. Then the diagrams of Figs. 3 and 4 were evaluated for all intermediate states differing in energy by $2\hbar\omega$ from the model space. Antisymmetrized versions of the Coulomb and nuclear interactions were used so as to include all exchange diagrams.

In view of the complexity of the particle-hole contribution an explicit expression is given for the diagram shown in Fig. 4(d):

$$\Delta E(\text{ph}) = -\frac{1}{2\hbar\omega}(-1)^J \sum_{\bar{J}} (2\bar{J}+1)\begin{Bmatrix} j_2 & \bar{J} & j_1 \\ j_3 & J & j_4 \end{Bmatrix} \sum_{\text{ph}} (-1)^{j_p+j_n} \sum_I (-1)^I \begin{Bmatrix} j_p & I & j_2 \\ j_1 & \bar{J} & j_h \end{Bmatrix} \langle 2p|K_1|1h\rangle_I (2I+I)$$

$$\times \sum_{I_C} (-1)^{I_C}\begin{Bmatrix} j_3 & I_C & j_p \\ j_h & J & j_4 \end{Bmatrix}\langle p3|v_C|h4\rangle_{I_C}(2I_C+1), \tag{8}$$

where $\begin{Bmatrix} a & b & c \\ d & e & f \end{Bmatrix}$ is the $6j$ symbol.[12] In this expression K_1 is the ^1S $(T=1)$ part of the nuclear residual interaction, and the energy $\Delta E(\text{ph})$ is for Ne^{18}. To deduce the corresponding F^{18} p-h energies Eq. (8) must be divided by 2 and K_1 replaced by $\frac{1}{2}(K_1+K_0)$, where K_0 is the ^3S $(T=0)$ interaction. To simplify calculation K_0 was set equal to $(1+\xi)K_1$, with $\xi_1 = \frac{1}{2}$, a reasonable value. The summed corrections, shown in Table VIII, are by no means negligible. The energies resulting from a rediagonalization of F^{18} and Ne^{18} are given in Table IX, and may be considered a slight improvement on the previous calculations. Tables VII and IX indicate for F^{18} a systematic upward shift of the lowest-lying state of each angular momentum. It will be argued in the next section that this is evidence for a charge dependence of non-Coulombic origin in the nuclear interaction.

IV. CHARGE DEPENDENCE IN THE NUCLEAR FORCE

Perhaps the most interesting aspect of a calculation such as the present one is the possibility of revealing the presence of a charge dependence in the basic nuclear force. The np, ^1S interaction has been demonstrated[13] to contain an additional attractive component. From the purely nucleon-nucleon data it is difficult to extract the exact

nature of this component, i.e., its range and strength, but a not unreasonable estimate of its strength is some 1 to 3% of the volume integral of the charge-independent low-energy ^1S force. The F^{18} calculations will be redone including an attractive zero-range force whose radial integral is 1.8% of that of the attractive component of the renormalized $K(E)$. The results are displayed in Table X and the improvement in agreement with experiment is striking. The zero-range nature of the additional force and the figure of 1.8% for the volume integral are in agreement with the charge dependence employed by Bertsch and Kahana[14] in a calculation of the T_z^3 term in the isobaric-mass equation for the $A=9$ nuclei. The np charge dependence played an important role in the latter calculation, contributing one-half the T_z^3 coefficient. Changing the range of the force to a value kept small in comparison to the size ($\gtrsim 3.2$ fm) of the $A=18$ valence orbits would not appreciably alter the above results, but too long a range would depress the 2_1^+ state considerably more. Of course the exact figure of 1.8% was determined to approximately fit the ground-state discrepancy in F^{18}, but the shifts obtained for the other states are true predictions.

The small np force introduced above destroys the charge independence of $K(E)$ but does not dis-

TABLE VII. Predicted and experimental binding energies $B(J_\alpha)$ and energy shifts $\Delta E(J_\alpha)$ for F^{18} and Ne^{18}. These are preliminary results prior to the inclusion of corrections from Figs. 3 and 4.

| | F^{18} | | | Ne^{18} | |
State	Calculated	Experimental	pp Coulomb	nn Coulomb	Experimental
			Binding energies $B(J_\alpha)$		
0^+_1	−3.868	−3.964	−3.379	−3.346	−3.320
0^+_2	−0.524	−0.266	−0.433	−0.390	0.256
2^+_1	−1.936	−1.947	−1.564	−1.535	−1.433
2^+_2	+0.012	−0.043	0.285	0.305	0.296
4	−0.344	−0.356	0.025	0.040	0.056
			Energy shifts $\Delta E(J_\alpha)$		
0^+_1	+0.035	−0.062	+0.523	0.556	0.582
0^+_2	−0.216	+0.002	−0.125	−0.082	0.524
2^+_1	−0.015	−0.025	0.359	0.388	0.489
2^+_2	−0.072	−0.057	0.201	0.221	0.282
4^+	+0.006	−0.006	0.375	0.390	0.406

turb charge symmetry. A difference in the nn and pp ^1S forces would in principle show up in the Ne^{18} spectrum. The two-body evidence for an appreciable charge asymmetry is weaker than for the np charge dependence.[13] Theoretical models are not likely to produce as large a charge asymmetry, because of the absence of the one-charged pion exchange in the nn or pp systems. Nevertheless, Negele[5] has suggested the existence of an additional rather strong repulsive pp force as an explanation for the single-particle difficulties mentioned earlier in this paper and elsewhere.[3, 4] The addition of such a term to our Ne^{18} calculations would not systematically improve the agreement with experiment obtained in Table IX. The agreement with the ground state would be disturbed, while any improvement in the 2^+ states is probably illusory in light of our discussion of single-particle energies.

V. ALTERNATIVE TWO-PARTICLE CALCULATIONS

In this section we discuss the effect of various alterations in our approach. Perhaps the greatest uncertainty is attached to our treatment of the single-particle energies in F^{18} and Ne^{18}. The reduction in the $d_{5/2}$-$s_{1/2}$ splitting from 870 keV in O^{17} to 500 keV in F^{17} was chiefly responsible for the unobserved depression of the second 0^+ state in Ne^{18} and F^{18} and to a lesser extent a depression of the 2^+ states in Ne^{18}. By binding the s and d nu-

cleons more deeply in the two-particle nuclei one may eliminate this difficulty. Such a step could be viewed as an attempt to introduce the correct asymptotic behavior into the two-particle wave functions. To this end the calculations of Secs. III B and III C are redone using the single-particle potentials of Table II, with increased neutron binding energies of −5.14 and −4.14 MeV for the d and s states, respectively. The single-particle proton d-s separation is taken to be the 0.617 MeV of Table II and of course the two-particle matrix elements, both Coulomb and nuclear, are altered. The results of this calculation are shown in Table XI. The comparison with experiment here must be considered excellent. Even the position of the troublesome 0^+_2 level has been improved.

TABLE VIII. Summed corrections to nuclear matrix elements from the diagrams of Figs. 3 and 4, excluding the already estimated contributions.

Angular momentum	State	Ne^{18} (keV)	F^{18} (keV)
0^+	$(d^2)^2$	72.3	24.8
0^+	d^2s^2	29.4	9.4
0^+	$(s^2)^2$	−21.0	−10.6
2^+	$(d^2)^2$	12.1	4.6
2^+	$d^2(ds)$	10.6	4.7
2^+	$(ds)^2$	12.8	5.5
4^+	$(d^2)^2$	2.5	0.8

TABLE IX. Corrected values $B(J_\alpha)$, $\Delta E(J_\alpha)$ including all dominant corrections from Figs. 3 and 4. Again the Ne^{18} results are displayed for a perturbative (nn) and an exact calculation (pp) of the Coulomb energy [Fig. 3(b)].

		$B(J_\alpha)$		
		Ne^{18}		
State	F^{18}	pp Coulomb	nn Coulomb	
0^+_1	−3.843	−3.305	−3.271	
0^+_2	−0.535	−0.456	−0.414	
2^+_1	−1.926	−1.540	−1.513	
2^+_2	0.013	+0.287	0.307	
4^+	−0.343	0.027	0.042	

	$\Delta E(J_\alpha)$				
	F^{18}		Ne^{18}		
State	Calculated	Experimental	pp Coulomb	nn Coulomb	Experimental
0^+_1	+0.060	−0.062	0.598	0.632	0.582
0^+_2	−0.227	+0.002	−0.148	−0.106	0.524
2^+_1	−0.005	−0.025	0.381	0.408	0.489
2^+_2	−0.071	−0.057	0.203	0.223	0.282
4^+	+0.007	−0.006	0.377	0.392	0.406

TABLE X. The F^{18} calculations redone including a charge dependence in the form of a zero-range force whose volume integral is 1.8% of the attractive component of the renormalized $K(E)$ of Eq. (4).

State	$B(J_\alpha)$ F^{18} (with 1.8% δ function)
0^+_1	−3.965
0^+_2	−0.553
2^+_1	−1.963
2^+_2	0.009
4^+	−0.354

State	$\Delta E(J_\alpha)$ F^{18} (with 1.8% δ function)	Experimental
0^+_1	−0.062	−0.062
0^+_2	−0.245	+0.002
2^+_1	−0.041	−0.025
2^+_2	−0.075	−0.057
4^+	−0.004	−0.006

A second approach to treating the single-particle energies is to completely ignore the F^{17} evidence and use the same d-s splitting in the three nuclei O^{18}, F^{18}, and Ne^{18}. If the mixed Coulomb-nuclear effects of Figs. 3 and 4 are retained, the predictions diverge greatly from experiment. However, if both the changes in single-particle energies and wave functions are ignored, the spectra obtained for F^{18} and Ne^{18}, Table XII, does not differ greatly from those of earlier calculations. Now, however, the 0^+_2 state is better positioned in the np nucleus with a residual disagreement in the pp nucleus.

One of the purposes of carrying out this work was to shed some light on the possible presence of a repulsive core in the residual interaction. In the calculation of purely nuclear energies, i.e., ignoring the role of the Coulomb energies, only matrix elements within the model space are of importance. To calculate the Coulomb effects discussed here, matrix elements to other shells are important. This is evident if one views the proton wave functions as expansions in a complete set of neutron wave functions derived from the charge-independent potential $U(\vec{r})$. It is also evident in the diagrams of Figs. 3 and 4. We have seen that there is some cancellation, in the final energies, between the Coulomb effects on single-particle energies and on two-particle matrix ele-

ments. There is also at play[1] a cancellation in the mixed nuclear-Coulomb energies themselves, between the repulsive and attractive parts of $K(E)$. In Fig. 3(c), for example, a repulsive nuclear force leads to an attractive contribution, an attractive force to a repulsive contribution. Because of its shorter range,[1] the repulsive component plays a more important role in Fig. 3(c) than it does in the purely nuclear matrix element. To highlight the relevance of the repulsive part of the force a final calculation was performed using only the attractive first term in Eq. (4), with its strength readjusted to again fit the O^{18} spectrum. The results for the ground states of Ne^{18} and F^{18} are unambiguous. The ground state of Ne^{18}, for example, now lies at -3.127 MeV, some 200 keV above its experimental position. Higher-angular-momentum states seem less sensitive to the presence of the repulsion, with the position of the 2_1^+ state in Ne^{18} being perhaps a bit improved.

VI. CONCLUSIONS

After the completion of the above calculations the situation is good but perhaps not so clear as one would desire. The results for four of the five $T = 1$ multiplets considered are very good. Theoretical changes in matrix elements due to mixed nuclear-Coulomb effects totalling some hundreds of keV lead to predictions, on occasion, of level shifts within tens of keV. The addition of the many corrections seems to improve the predictions, and

there is reasonable evidence for the presence of an attractive charge dependence in the $A = 18$ system of the sort expected from purely two-body data. However, the failure to position the second 0^+ level in F^{18}, Ne^{18} is somewhat of a mystery. The simple-minded approach of ignoring single-particle effects can go some way toward correcting the 0^+ discrepancy but is hardly in line with one's view of a consistent shell-model calculation. It must be pointed out that the experiments[10] which extract the $T = 1$ states in F^{18} from the $T = 0$ background are difficult. The direct reactions identifying the second 0^+ state all possess small cross sections to this state and only poorly pin down its label as a predominantly $(2s_{1/2})^2$ state. Nevertheless most shell-model calculations with realistic residual interactions do place a state of this nature at more or less the energy at which it is seen. The Ne^{18} experiments[11] are, in principle, easier to perform in the absence of the $T = 0$ background. The additional electromagnetic evidence in O^{18} that the shell model fails badly in predicting the size of the transition from 0_2^+ to 2_1^+ suggests one can expect a considerable amount of core excitation in this state. Also the calculations of Buck, McGrory, and Zuker[15] indicate a relatively large amount of core excitation in all the states we considered. A natural extension of the present calculation is to include the Coulomb-induced corrections in the matrix elements of this last reference. It will be interesting to see if the successful results of this work can be retained, while bringing

TABLE XI. The F^{18}, Ne^{18} binding energies and shifts from O^{18} energies calculated using the more deeply bound single-particle levels of Table II, and including the corrections of Figs. 3 and 4. The comparison with experiment must be considered good. The position of the troublesome 0_2^+ level has been improved somewhat.

State (J^π)	O^{18}	$B(J_\alpha)$ F^{18}	(with 1.4% δ function)	Ne^{18} pp Coulomb	nn Coulomb
0_1^+	-3.901	-3.865	-3.961	-3.334	-3.311
0_2^+	-0.300	-0.462	-0.475	-0.293	-0.263
2_1^+	-1.924	-1.923	-1.953	-1.511	-1.489
2_2^+	0.094	0.043	0.040	0.342	0.358
4^+	-0.350	-0.345	-0.353	0.035	0.047

State	$\Delta E(J_\alpha)$ F^{18} (with 1.4% δ function)	Experimental	pp Coulomb	Ne^{18} nn Coulomb	Experimental
0_1^+	-0.060	-0.062	0.567	0.590	0.582
0_2^+	-0.175	$+0.002$	$+0.015$	$+0.045$	0.524
2_1^+	-0.029	-0.025	0.413	0.435	0.489
2_2^+	-0.054	-0.057	0.248	0.264	0.282
4^+	-0.003	-0.006	0.385	0.397	0.406

TABLE XII. The $B(J_\alpha)$ and $\Delta E(J_\alpha)$ deduced by ignoring changes in single-particle energies and in nuclear two- particle matrix elements. The shifts in F^{18} come purely from a np charge-dependent force and in Ne^{18} from including the two-particle Coulomb energy of Fig. 3(b).

| | $B(J_\alpha)$ | | | |
| | F^{18} | | Ne^{18} | |
State	(with 1% δ function)	Experimental	pp Coulomb	Experimental
0_1^+	−3.971	−3.964	−3.442	−3.320
0_2^+	−0.318	−0.266	0.005	0.256
2_1^+	−1.941	−1.947	−1.528	−1.433
2_2^+	0.081	−0.043	0.254	0.296
4^+	−0.356	−0.356	0.013	0.056

| | $\Delta E(J_\alpha)$ | | | |
| | F^{18} | | Ne^{18} | |
State	(with 1% δ function)	Experimental	pp Coulomb	Experimental
0_1^+	−0.069	−0.062	0.461	0.582
0_2^+	−0.010	+0.002	0.313	0.524
2_1^+	−0.020	−0.025	0.393	0.489
2_2^+	−0.003	−0.043	0.170	0.282
4^+	−0.006	−0.006	0.363	0.406

the 0_2^+ level more into line. Introducing core polarization into the wave functions will have the effect of making all states less sensitive to single-particle Coulomb changes.

It is clear from this work that the Coulomb energy shifts in $T=1$ multiplets are sensitive to the nuclear interaction. If one is trying to elicit the nature of this interaction then this sensitivity is all to the good. However, it will be necessary to redo the calculations with a variety of interactions; in particular, to allow a force in other than the ^1S partial wave.

Similar calculations may be performed in other regions of the Periodic Table. An apparently ideal $T=1$ set of multiplets to examine are the states of the $A=42$ nuclei, Ca^{42}, Sc^{42}, Ti^{42}. Unfortunately the $p_{3/2}$ proton in Sc^{41} is unbound, and a simple shell-model calculation including this state still is out of the question. The $d_{3/2}$ state for $A=18$ was left out of the present calculations for similar reasons. (Attempts to estimate the effect of including this state indicated little change in the five $A=18$, $T=1$ multiplets.) A purely $f_{7/2}^2$ treatment of the $A=42$ ground states is quite successful and again required a np charge dependence of some 2% in volume integral.

Finally we have concentrated only on the energy shifts of states and not on changes in wave functions. This separate problem and the obviously connected problem of isospin admixtures will be

considered in a future work. For the present, however, it is interesting to present the changes in "model" wave functions induced by the Coulomb effects. For example, these wave functions for the 0_1^+ states in the $A=18$ nuclei are:

$$\Psi_M(O^{18}) = 0.8930(d^2)^0 + 0.4500(s^2)^0,$$

$$\Psi_M(F^{18}) = 0.8858(d^2)^0 + 0.4640(s^2)^0,$$

$$\Psi_M(Ne^{18}) = 0.8692(d^2)^0 + 0.4945(s^2)^0.$$

The overlap of the Ne^{18}, F^{18} wave functions is 0.985, despite the differing amounts of s^2 and d^2 they possess. It is this overlap which would enter into the superallowed β decay between the ground state of Ne^{18} and the lowest $T=1$ state in F^{18}. Of course, a consistent treatment of the wave functions must include the pieces from the non-model part of Hilbert space.

VII. ACKNOWLEDGMENTS

*Work performed under the auspices of the U. S. Atomic Energy Commission.

[1]E. H. Auerbach, S. Kahana, C. K. Scott, and J. Weneser, Phys. Rev. 188, 1747 (1969).

[2]S. Kahana, H. C. Lee, and C. K. Scott, Phys. Rev. 180, 956 (1969).

[3]J. A. Nolen and J. P. Schiffer, Phys. Letters 29B, 396 (1969).

[4]E. H. Auerbach, S. Kahana, and J. Weneser, Phys. Rev. Letters 23, 1253 (1969).

[5]J. Negele, to be published.

[6]R. G. Thomas, Phys. Rev. 88, 1109 (1952).

[7]K. Brueckner, Phys. Rev. 97, 1353 (1955); H. A. Bethe and J. Goldstone, Proc. Roy. Soc. (London) A238, 551 (1957); C. W. Wong, Nucl. Phys. A104, 417 (1967); T. T. S. Kuo and G. E. Brown, Nucl. Phys. 85, 40 (1966); S. Kahana, H. C. Lee, and C. K. Scott, Phys. Rev. 185,

1378 (1969).

[8]S. Kahana and E. Tomusiak, Nucl. Phys. 71, 402 (1965).

[9]T. T. S. Kuo and G. E. Brown, Nucl. Phys. 85, 40 (1966).

[10]L. M. Polsky, C. H. Holbrow, and R. Middleton, Phys. Rev. 186, 966 (1969).

[11]B. C. Robertson, R. A. I. Bell, J. L'Ecuyer, R. D. Gill, and H. J. Rose, Nucl. Phys. A126, 431 (1969).

[12]M. Rotenberg, R. Bivins, N. Metropolis, J. K. Wooten, Jr., The Technology Press, MIT, Cambridge, Massachusetts (1959).

[13]E. M. Henley, in Isospin in Nuclear Physics, edited by D. H. Wilkinson (North-Holland, Amsterdam, 1969).

[14]G. Bertsch and S. Kahana, Phys. Letters 33B, 193 (1970).

[15]B. Buck, J. B. McGrory, and A. Zuker, Phys. Rev. Letters 21, 39 (1968).

Bethe-Goldstone Equation in Finite Nuclei*

Joslyn R. Demos† and Manoj K. Banerjee

Department of Physics and Astronomy, University of Maryland, College Park, Maryland 20742

(Received 15 July 1971)

Following Brandow's suggestion of setting $QUQ = 0$, where U is the single-particle potential, the Bethe-Goldstone equation becomes $\Psi = \Phi - [Q/(QTQ - \omega]v\Psi$. This equation has been approximated by replacing Q with the Eden-Emery Pauli operator and by neglecting $\hat{T}\chi$, where $\hat{T}$ is the off-diagonal part of the c.m. kinetic energy operator in the oscillator representation. Care has been taken to retain $\hat{T}\Phi$, which is a large term. The approximate equation has been solved iteratively. It yields defect functions with the bulk of the effect of Q built in. Correction terms to our approximate results have been estimated. A very satisfactory feature of the present approach is that there is considerable cancellation between the so-called spectral and Pauli correction terms. The biggest correction term is $\langle \chi | \hat{T} | \chi \rangle$, which can be as large as 0.5 MeV in the triplet even case.

1. INTRODUCTION

The Bethe-Goldstone equation, which is a device to sum ladder diagrams, plays a central role in the Brueckner-Bethe approach to the nuclear many-body problem. It has the form[1]

$$\Psi = \Phi - \frac{Q}{H_0 - \omega} v\Psi . \tag{1}$$

v is the free nucleon-nucleon interaction potential. ω is the starting energy determined by the main diagram of which the ladder may be a part. H_0 is an independent-particle Hamiltonian. The space of the eigenfunctions of this Hamiltonian is divided into two parts. The low-lying part is the model space, and the remainder is usually called the intermediate space. Φ is a product of two single-nucleon wave functions from the model space, and Ψ is the correlated two-nucleon wave function. Q is the projection operator onto the space where both nucleons are in the immediate space.

The Hamiltonian H_0 is the sum of the kinetic energy operator T of the two nucleons and a single-particle potential U. The latter is chosen to cancel as many diagrams as possible. Considerable attention has been paid to the question of the optimum choice of U. The most notable is the work of Brandow.[2]

In the definition of the potential, there is an inherent asymmetry between the treatment of the states in the model space and that of the intermediate states. Thus, while a bubble insertion on a hole line [Fig. 1(a)] can be put "on shell," i.e., made independent of the rest of the diagram of which the hole line is a part, the same cannot be done for the bubble insertion on a particle line. As a result, the diagram of Fig. 1(a) can be canceled by U quite easily, while one could only hope to do the same for Fig. 1(b) in an average sense. Moreover, Bethe[3] and Rajaraman[4] pointed out that there are many other diagrams which are likely to be as important as Fig. 1(b), and these should be